



Accurate quantification of mouse mitochondrial DNA without co-amplification of nuclear mitochondrial insertion sequences

Afshan N. Malik *, Anna Czajka, Phil Cunningham

Diabetes Research Group, Division of Diabetes and Nutritional Sciences, School of Life Science and Medicine, King's College London, SE1 1UL, UK

ARTICLE INFO

Article history:

Received 22 January 2016

Received in revised form 3 May 2016

Accepted 11 May 2016

Available online 12 May 2016

Keywords:

Mitochondrial DNA

Mitochondrial pseudogenes

NumtS

Real time PCR

Mouse mitochondrial genome

ABSTRACT

Background: Mitochondria contain an extra-nuclear genome in the form of mitochondrial DNA (MtDNA), damage to which can lead to inflammation and bioenergetic deficit. Changes in MtDNA levels are increasingly used as a biomarker of mitochondrial dysfunction. We previously reported that in humans, fragments in the nuclear genome known as nuclear mitochondrial insertion sequences (NumtS) affect accurate quantification of MtDNA. In the current paper our aim was to determine whether mouse NumtS affect the quantification of MtDNA and to establish a method designed to avoid this.

Methods: The existence of NumtS in the mouse genome was confirmed using blast N, unique MtDNA regions were identified using FASTA, and MtDNA primers which do not co-amplify NumtS were designed and tested. MtDNA copy numbers were determined in a range of mouse tissues as the ratio of the mitochondrial and nuclear genome using real time qPCR and absolute quantification.

Results: Approximately 95% of mouse MtDNA was duplicated in the nuclear genome as NumtS which were located in 15 out of 21 chromosomes. A unique region was identified and primers flanking this region were used. MtDNA levels differed significantly in mouse tissues being the highest in the heart, with levels in descending order (highest to lowest) in kidney, liver, blood, brain, islets and lung.

Conclusion: The presence of NumtS in the nuclear genome of mouse could lead to erroneous data when studying MtDNA content or mutation. The unique primers described here will allow accurate quantification of MtDNA content in mouse models without co-amplification of NumtS.

© 2016 Elsevier B.V. and Mitochondria Research Society. All rights reserved.

1. Introduction

Mitochondria are eukaryotic organelles in the cytosol of eukaryotic cells whose main function is to generate energy in the form of ATP, and regulate key cellular functions including the redox state of cells, apoptosis, calcium homeostasis, cellular differentiation and growth (Chan, 2006; Green and Reed, 1998). The numbers of mitochondria can vary from hundreds to thousands per cell, depending on the cell's bio-energetic requirements (Hock and Kralli, 2009; Williams, 1986).

Mitochondria contain their own circular DNA genome, and as each mitochondrion can contain 2–10 copies of 5- μ m circular mitochondrial DNA genome, cells with mitochondria contain hundreds to thousands of copies of MtDNA per nuclear genome (Bogenhagen, 2012). MtDNA is transcribed and translated within the mitochondrion and its replication is independent of phase-restricted nuclear DNA and the cell cycle and responds to physiological stimuli (Falkenberg et al., 2007). It is generally

assumed that MtDNA level correlate with both mitochondrial function, and the number of mitochondria in the cell (Hock and Kralli, 2009; Williams, 1986). However, altered MtDNA levels associated with disease in blood samples, body fluids, and cells and tissues have been reported in a wide range of human diseases leading to the hypothesis that changes in MtDNA content may be indicative of mitochondrial dysfunction (Malik and Czajka, 2013). Alterations in MtDNA may be indicative of altered metabolic activity; or they can also be indicative of potential inflammatory pathways, as MtDNA has emerged as a mediator of inflammation as if in the wrong place, it can activate immune responses because of the resemblance to bacterial DNA (Arnoult et al., 2011; Zhang et al., 2010).

The mitochondrial genome comprises of 16,569 base pairs (bp) in humans and between 16,301–16,769 bp in mouse (Wallace and Fan, 2009). MtDNA is highly conserved between organisms and encodes 37 genes; 13 mRNAs, 2 rRNAs and 22 tRNAs and 1 non-coding D-loop region (Falkenberg et al., 2007). The remainder of more than 1500 mitochondrial proteins are encoded by nuclear genome, transcribed into mRNAs, translated on cytoplasmic ribosomes, and imported into the mitochondrion (Schatz, 1996). Fragments of mitochondrial genome are present in the nuclear genome in the form of pseudogenes called

Abbreviations: MtDNA, mitochondrial DNA; NumtS, nuclear mitochondrial insertion sequence.

* Corresponding author.

E-mail address: afshan.malik@kcl.ac.uk (A.N. Malik).

NumtS (Nuclear mitochondrial insertion sequences), which have been found to lead to erroneous identification of mitochondrial heteroplasmies (Wallace et al., 1997; Yao et al., 2008).

The quality and quantity of MtDNA is widely employed as a determinant of mitochondrial activity. The most commonly used method used to measure MtDNA content in a cell is to quantify the mitochondrial genome versus nuclear genome ratio, termed Mt/N (Ajaz et al., 2015; Malik and Czajka, 2013; Malik et al., 2009; Malik et al., 2011). The problem with MtDNA quantification methods is that co-amplification of NumtS is likely to lead to erroneous data when measuring MtDNA content or the presence of MtDNA mutations. Furthermore, southern blot based methods are still in use (Bayona-Bafaluy et al., 2005) which are likely to lead to cross hybridisation of NumtS rather than specifically MtDNA. To overcome this issue, we previously developed a PCR-based method by identifying unique regions in the human mitochondrial genome not duplicated in the nuclear genome to accurately quantify MtDNA from human samples (Malik et al., 2011). However, a similar approach has not been described for mouse MtDNA, and there is little information in the literature about whether mouse MtDNA is present as NumtS in the nuclear genome. Therefore, in the current paper our objective was to investigate the presence of NumtS in the mouse nuclear genome, define regions in the mouse mitochondrial genome which are unique and not duplicated in the nuclear genome, and to use primers designed to these in order to accurately measure MtDNA copy numbers in a range of mouse tissues.

2. Material and methods

2.1. Identification of unique regions of mitochondrial genome and primer design

The duplication of the mitochondrial genome in the nuclear genome was detected using BLAST version 2.2.32 (<http://www.ncbi.nlm.nih.gov>) (Pearson and Lipman, 1988). Unique regions were identified in the mouse mitochondrial sequence, retrieved from ENSEMBL (Flicek et al., 2010) using FASTA version 3.5.2.7 (Altschul et al., 1990) as described previously (Malik et al., 2011). To measure nuclear DNA, primers against single copy nuclear gene, beta-2 microglobulin (B2M) were designed (Table 1).

2.2. Animals

Male C57BL/6 mice (Charles River, Margate, UK) were kept in standard conditions. All animal procedures were approved by our institution's Ethics Committee and carried out under license, in accordance with the UK Home Office Animals (Scientific Procedures) Act 1986. Animals were sacrificed when they reached 3 months of age according to approved protocols and tissue and blood samples of these mice were collected and immediately snap frozen. Samples were stored at -80°C .

2.3. Genomic DNA preparation

Tissue samples were homogenized using TissueLyser (Qiagen) in order to eliminate cross-contamination. Total genomic DNA was extracted using the DNeasy Blood & Tissue kit according to manufacturer's instruction (Qiagen) (Malik et al., 2011). Before proceeding to qPCR, the

DNA template was subjected to the pre-treatment (DNA template shearing using bath sonicator Kerry, Pulsatron 55 which uses $38\text{ kHz} \pm$ for 10 min) as described previously (Ajaz et al., 2015; Malik et al., 2011) in order to avoid dilution bias. The template concentration was determined using NanoDrop and adjusted to $10\text{ ng}/\mu\text{l}$. To avoid errors arising from repeated freeze thaw cycles DNA samples were kept at 4°C for the duration of study.

2.4. Real-time PCR

MtDNA content was assessed by absolute quantification using real time PCR. Primers for mouse MtDNA (mMitoF1, mMitoR1) and mouse B2M (mB2MF1, mB2MR1) were used to amplify the respective products from mouse genomic DNA (Table 1). PCR products were purified and used to prepare dilution standards for both amplicons and the range of dilutions used were 10^2 – 10^8 copies per $2\text{ }\mu\text{l}$ to allow absolute quantification. MtDNA copy number per cell were determined from template DNA by carrying out qPCR in a total volume of $10\text{ }\mu\text{l}$, containing $5\text{ }\mu\text{l}$ of Quantifast SYBR Master Mix (Qiagen), $0.5\text{ }\mu\text{l}$ of forward and reverse primer (400 nM final concentration each), $2\text{ }\mu\text{l}$ template DNA and $2\text{ }\mu\text{l}$ of DNase free water. The reactions were performed in Roche LightCycler (LC) 480 instrument using the following protocol: pre-incubation at 95°C for 5 min (1 cycle); denaturation at 95°C for 10 s, annealing and extension at 60°C for 30 s (repeat denaturation and extension steps for 40 cycles), melting at 95°C for 5 s, 65°C for 60 s, and 95°C continues (melt curve analysis: 1 cycle) and the last step, cooling at 40°C for 30 s. The specificity of the primers (one PCR product amplified) was confirmed as a single melt peak and single band when electrophoresed on 2% agarose gel for both amplicons (not shown). qPCR efficiency calculated from the slope was between 95 and 105% with co-efficiency of reaction $R^2 = 0.98$ – 0.99 .

3. Results

3.1. Identification of nuclear mitochondrial insertion sequences (NumtS) in the mouse genome

We used the mouse mitochondrial genome sequence (accession number NC_005089.1) derived from *Mus musculus* (Goios et al., 2007) and which shows high sequence identity with mitochondrial genomes from commonly used mouse strains, to search for similar sequences in the mouse nuclear genome reference sequence using blast (NCBI, <http://blast.ncbi.nlm.nih.gov/Blast.cgi> *Mus musculus*). The resulting data showed that many regions of the mouse mitochondrial genome showed strong sequence identity ($>90\%$) with regions located in the nuclear genome, suggesting that these regions contain NumtS (Fig. 1a). NumtS were found in 15 out of 21 mouse chromosomes and ranged from 30 bp to 4654 bp (Fig. 1b). More than 95% of the mouse mitochondrial genome was present in varying lengths and different positions in the mouse nuclear genome.

3.2. Design of unique primers to amplify mouse mitochondrial DNA

The mouse mitochondrial genome sequence was split into overlapping fragments of 150 bp length with a 50 bp overlap at each end, and each fragment was used as a query sequence in a FASTA search against the entire mouse genome, one chromosome at a time (both strands).

Table 1
Oligonucleotides used in the study.

Accession number	Primer	Oligonucleotide sequence (5' → 3')	Product size (bp)
NC_005089.1	mMitoF1	CTAGAAACCCCGAAACCAAA	125
	mMitoR1	CCAGCTATCACCAAGCTCGT	
NC_000068.7	mB2MF1	ATGGGAAGCCGAACATACTG	177
	mB2MR1	CAGTCTCAGTGGGGGTGAAT	

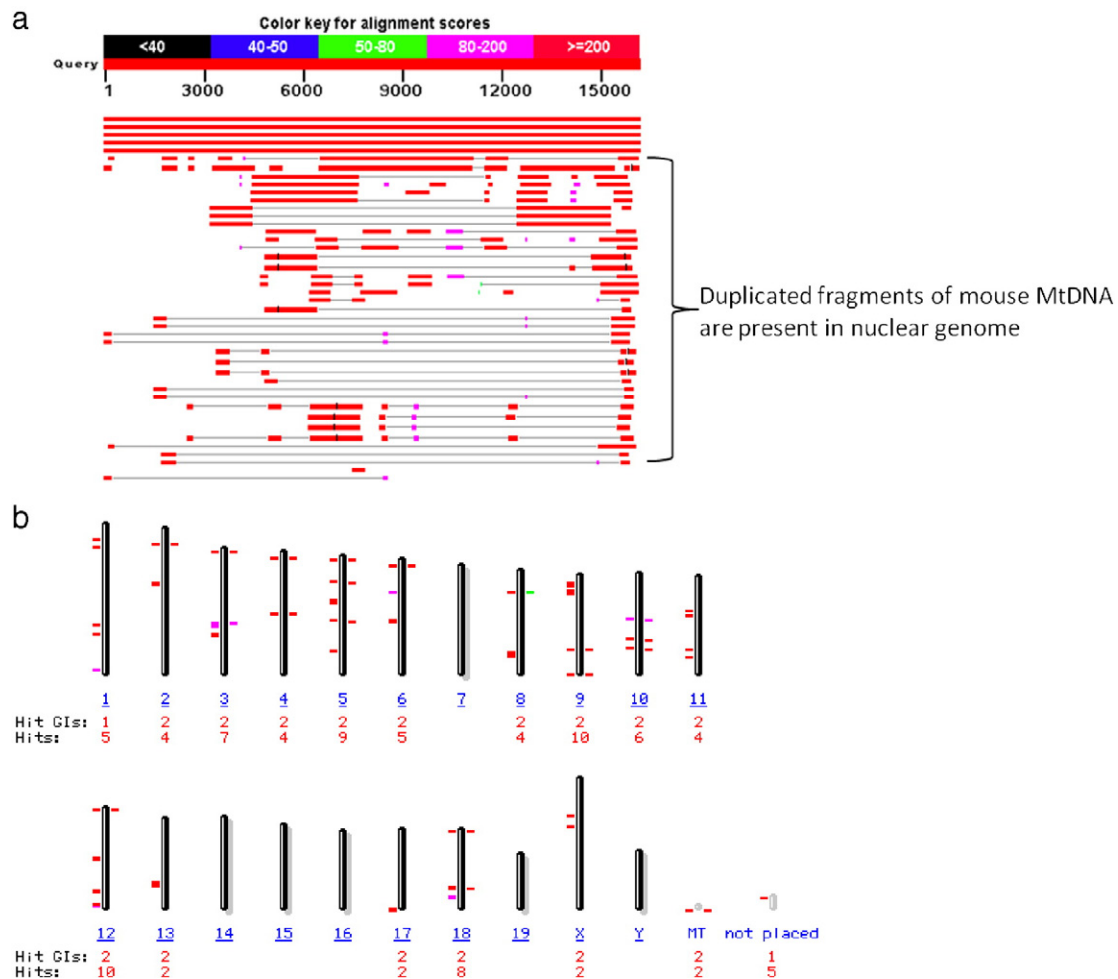


Fig. 1. Duplication of mouse mitochondrial genome in nuclear genome. (a) The thick red line (query) representing the mitochondrial genome sequence accession number NC_005089.1, was blasted against the reference sequence of the mouse genome using blastn, the first 40 best matching sequences are shown, top 5 red lines being an exact match to the mitochondrial genome, whereas the remaining 35 lines are regions of the nuclear genome showing a high degree of identity. The colour key for alignment scores is given at the top of the figure with red being the highest alignment score. (b) Mitochondrial pseudogenes in the nuclear genome are shown as bars against the relevant mouse chromosome, the extent of the homology is shown as a colour code indicated in and the number of hits is shown in red numbers below the chromosome number shown in blue.

Each candidate 'unique' sequence was tested using BLAST to ensure programmatic accuracy. Using this approach, a unique mitochondrial sequence of 211 bp was identified, this region flanks position 1323–1447 of the mouse mitochondrial genome (accession number NC_005089.1), and accounts for less than 1.5% of the whole mouse mitochondrial genome. In addition, we found that between positions 200–3000 of the mouse mitochondrial genome, the frequency and length of NumtS were smaller and presence of other unique regions might be possible. We used the sequence at position 1323–1447 to design primers mMitoF1 and mMitoR1 which do not co-amplify NumtS (Table 1).

3.3. Absolute quantification of mouse mitochondrial DNA

The primers designed above were used to test the accuracy and reproducibility of the assay using mouse kidneys (Fig. 2). Total DNA isolated from kidneys of C57BL/6 mice ($n = 18$) was used as template for amplification and quantification of the two target regions using mMito and mB2M primers (Table 1). The template DNA was sonicated, the concentration adjusted to 10 ng/ μ l, and qPCR was carried out in triplicate for 10 ng and 1 ng per template, the resulting averages representing 6 measurements per original sample for each gene were used to calculate the mitochondrial genome to nuclear genome ratio in the samples (Table 2) and to test the accuracy of the assay (Fig. 2a). The amount of

mitochondrial and nuclear DNA in 10 ng and 1 ng, using values extrapolated from the standards curves, is shown in Fig. 2b and c respectively and shows that as expected, 10 fold reduction of the amount of template used results in 10-fold reduction of both MtDNA and B2M, i.e. removal of the dilution effect which can skew the Mt/N ratio (Malik et al., 2011). The Mt/N values in the samples remain constant (Fig. 2a) and melting curve analysis and DNA sequencing confirmed the specificity of the qPCR reactions (not shown).

We next used the assay to determine the accurate amount of MtDNA in a range of mouse tissues and blood samples (Fig. 3) as the mitochondrial genome to nuclear genome ratio. MtDNA was detected in all samples. The highest detected MtDNA copy number was in the heart (1273 copies/nuclear genome) followed by the kidney (332 copies/nuclear genome) and surprisingly, the lowest was in lung and islets (6 and 33 copies/nuclear genome respectively, Fig. 3).

4. Discussion

In this study, we have described the measurement of mouse MtDNA content using real-time qPCR and primers targeting a unique sequence in the mouse mitochondrial genome without co-amplification of mouse NumtS. We showed that more than 95% of the mitochondrial genome is duplicated in the mouse nuclear genome in the form of NumtS, with the

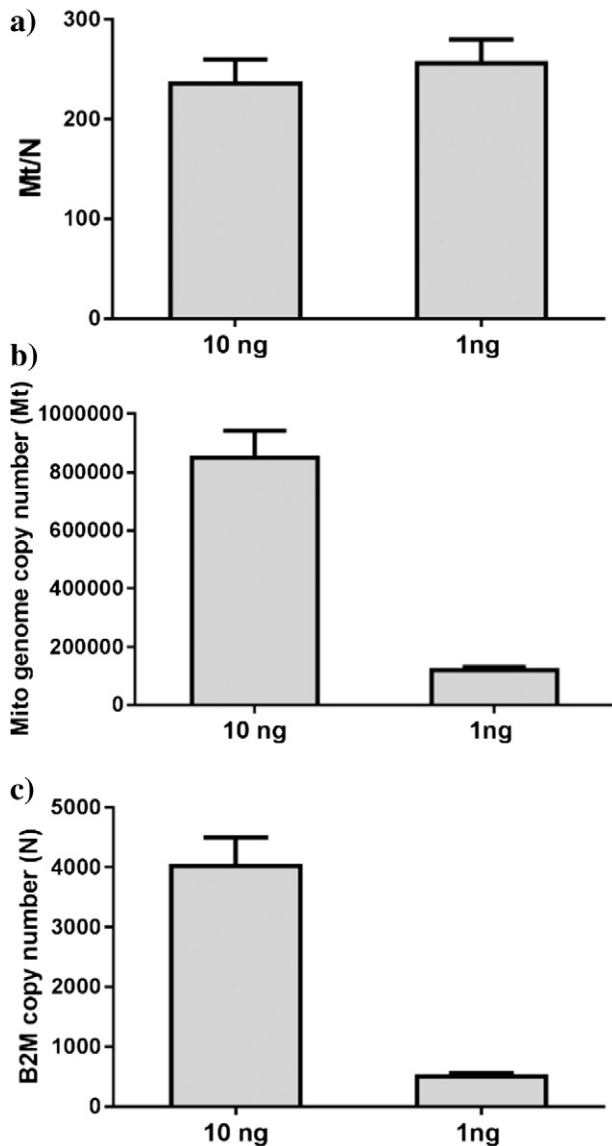


Fig. 2. Assay validation using different concentration of template. Mouse kidneys were collected from C57BL/6 mice ($n = 18$), total DNA was extracted, pre-treated and diluted to 10 ng/ μ l and 1 ng/ μ l. MtDNA content was quantified using absolute quantification with real-time qPCR. Data are shown for both 10 ng and 1 ng dilutions as mean values \pm SEM derived from Table 1. (a) MtDNA content (Mt/N) calculated as the ratio of mitochondrial genome to nuclear genome. (b) Absolute MtDNA copy numbers without normalisation to nuclear genome. (c) Absolute nuclear DNA copy numbers.

same MtDNA region being present in several chromosomal regions within the nuclear genome. Our observation is in accordance to a report by Richly and Leister, who demonstrated that mouse and human mitochondrial genomes have the highest ratio of NumtS in the nuclear genome (99% and 98% respectively) when compared with other eukaryotic genomes which generally have less than 50% of the transferred MtDNA pseudogenes (Richly and Leister, 2004). NumtS are usually fragmented and equally distributed among chromosomes (Woischnik and Moraes, 2002). Calabrese et al. reported that mouse NumtS are shorter, but much more conserved when compared to pseudogene sequences in chimpanzee and rhesus monkey (Calabrese et al., 2012).

We detected mouse NumtS in 15 out of 21 mouse chromosomes with the largest mouse Numt being identical to ~30% of mouse mitochondrial genome. The region of the mitochondrial genome located between position 200 and 3000 contained lower numbers of NumtS which

were also shorter in length allowing us to identify a unique region at position 1323 to 1447 which could be utilised for qPCR. The demonstration of NumtS in the mouse genome should be taken into account when detecting either mitochondrial mutations or measuring MtDNA content. The presence of NumtS in the nuclear genome has in the past led to erroneous reports of MtDNA mutations and of association with diseases (Wallace et al., 1997; Yao et al., 2008). It can also lead to errors in determination of MtDNA content when using primers targeting both MtDNA and NumtS (Wallace et al., 1997). Many studies use primers designed to target mitochondrial genes which are part of OXPHOS system (Goo et al., 2013; Guo et al., 2014; Stangenberg et al., 2015; Zhao and Chen, 2014). However, in mice, the entire sequences of cytochrome c oxidase I, II and III (Cox1, Cox2 and Cox 3), and 99% of the cytochrome b (Cyt b) sequence are duplicated in the mouse nuclear genome, and therefore likely to lead to erroneous data. It may be argued that co-amplification of mitochondrial NumtS may have no significant effect on overall results since some cells contain thousands of copies of MtDNA and only two copies of nDNA. However, when small disease associated changes are being reported potential errors could skew data, especially when one considers that the extraction method (Guo et al., 2009), storage and pre-treatment of the template (Malik et al., 2011) can cause an unequal distribution of the nuclear DNA and MtDNA in samples (Malik and Czajka, 2013). Many NumtS are presented several times in the nuclear genome and it has been suggested that their copy numbers can change with disease. For example, Caro et al. (2010) showed that mitochondrial sequences corresponding to cytochrome oxidase III and 16S rRNA were present in purified nuclei of liver and brain tissues from young and old rats. Interestingly, these regions contained the same SNPs found in the mitochondrial genome of the same age and their copy numbers increased with age. This study suggests that NUMTs are variable with age and is an additional reason to avoid using PCR procedures which amplify NUMTs (Caro et al., 2010). We suggest that attempts should be made to minimize experimental errors by ensuring that the target sequences are specific and that the protocols employed do not affect data due to co-amplification of NumtS, dilution bias or storage issues as described earlier (Guo et al., 2009; Malik et al., 2011). Our mtDNA quantification approach has undergone rigorous quality control. The assay is carried out at optimized template concentrations after template pre-treatment to enhance accuracy, ensuring that the “dilution effect” caused by the differing solubility of the mitochondrial genome versus the nuclear genome is minimized. The issues around template preparation and handling stem from the differing genome sizes, the mitochondrial genome is small and circular, the nuclear genome is large and comprised of linear fragments, and the two genomes have differing properties in solution resulting in skewing of the ratio. Therefore in the assay each target was measured using absolute quantification in triplicate at 2 different dilutions. The assay shows >99% primer specificity, quantity CV <5% plate to plate variability and has been validated by comparison of output from >4 independent lab workers.

MtDNA content has been shown to be altered in the variety of diseases in tissues and in circulating cells in human studies, and is a commonly used marker of mitochondrial health in animal studies, including diabetes (Bonnard et al., 2008; Liu et al., 2015; Supale et al., 2013), Parkinson's disease (Perier et al., 2013), and cancer (Morscher et al., 2015).

The unique primers which we describe here do not co-amplify mouse NumtS and therefore can be used to determine absolute copy numbers of MtDNA in a range of mouse tissues as well as in conditions of disease. We found that the tissues with the highest MtDNA content were heart and kidney, and surprisingly, the lowest MtDNA content was found in lung, being even lower than whole peripheral blood. These findings correlate with results reported by others in human (Mercer et al., 2011) and in rat tissues (Fernandez-Vizarra et al., 2011). It would be interesting to determine if MtDNA content in different organs and cell types is indicative of bioenergetic function, and whether tissues such as heart and kidney, which contain the highest

Table 2

Absolute quantification of mitochondrial DNA and nuclear DNA: comparison of data from two different dilutions of template DNA obtained from mouse kidneys. Columns 3–5 represent replicates of mitochondrial gene copy number, and columns 7–9 represent replicates of B2M copy number. Mitochondrial DNA content (MT/N ratio) is shown in column 11.

Animal number	DNA conc. (ng)	Mito1	Mito2	Mito3	Average	B2M1	B2M2	B2M3	Average	Mt/N
1	10	787,000	801,000	690,000	850,463	5230	4770	4460	4027	158
2	10	1,330,000	1,330,000	1,400,000		6340	5360	6590		222
3	10	1,580,000	2,130,000	ND		3370	3300	5490		458
4	10	1,120,000	1,200,000	1,110,000		5490	7060	6550		180
5	10	637,000	936,000	737,000		3300	3850	2720		234
6	10	913,000	871,000	1,230,000		5880	5120	5010		188
7	10	938,000	672,000	1,210,000		4730	4460	5590		191
8	10	925,000	925,000	1,200,000		5850	6400	6000		167
9	10	538,000	394,000	542,000		2450	1690	1040		285
10	10	714,000	688,000	471,000		3100	2630	2420		230
11	10	645,000	457,000	394,000		1810	989	1060		388
12	10	271,000	379,000	517,000		2016	1897			199
13	10	1,100,000	933,000	911,000		6860	6660	6150		150
14	10	585,000	585,000	409,000		3620	2860	4630		142
15	10	1,000,000	ND	860,000		7720	7600	6720		127
16	10	453,000	406,000	412,000		1500	1590	1490		278
17	10	1,300,000	1,130,000	1,140,000		2280	2770	2830		453
18	10	452,000	412,000	370,000		1750	2340	2120		199
1	1	99,100	84,700	85,300	118,469	291	422	561	503	211
2	1	166,000	180,000	244,000		707	1070	1110		204
3	1	142,000	157,000	177,000		376	202	256		571
4	1	99,400	100,400	99,400		823	768	849		123
5	1	112,000	149,000	154,000		460	540	679		247
6	1	181,000	170,000	156,000		537	877	475		268
7	1	84,700	71,900	118,000		477	587	838		144
8	1	252,000	196,000	209,000		727	605	727		319
9	1	20,300	77,500	60,500		179	133	181		321
10	1	68,500	74,800	72,600		300	345	395		208
11	1	65,400	62,500	60,300		276	233	209		262
12	1	67,500	65,000	63,300		163	240	259		296
13	1	131,000	126,000	213,000		621	388	531		305
14	1	146,400	139,300	151,500		640	538	673		236
15	1	142,000	138,000	185,000		878	1180	769		164
16	1	65,200	68,700	61,400		309	211	259		251
17	1	150,000	112,000	177,000		450	429	430		335
18	1	44,200	42,200	58,300		348	394	254		145

levels of MtDNA, are more prone to MtDNA damage and MtDNA mediated inflammation.

Acknowledgements

Thanks to Dr. Aileen King and Dr. Chloe Rackham for providing access to mouse tissues.

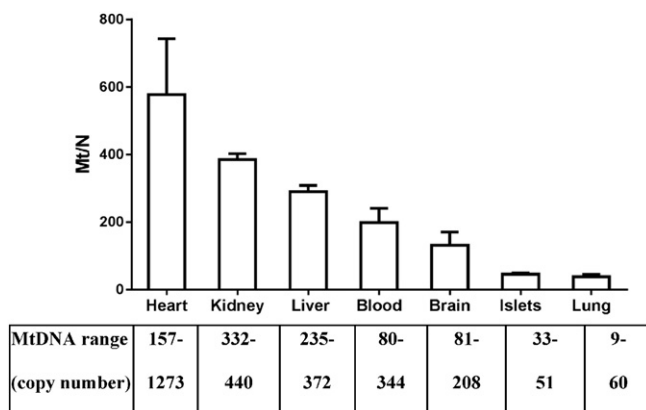


Fig. 3. Mitochondrial DNA copy numbers in mouse tissues. Tissue samples were collected from healthy control C57BL/6 mice. Following DNA extraction and template pre-treatment, MtDNA content was assessed as the ratio of mitochondrial genome to nuclear genome (Mt/N) using real-time qPCR. Data are shown as mean \pm SEM, n = 3–4 (brain and islets samples), and n = 6 for rest of tissues.

References

- Ajaz, S., Czajka, A., Malik, A.N., 2015. Accurate measurement of circulating mitochondrial DNA content from human blood samples using real-time quantitative PCR. *Methods Mol. Biol.* 1264, 117–131.
- Altschul, S.F., Gish, W., Miller, W., Myers, E.W., Lipman, D.J., 1990. Basic local alignment search tool. *J. Mol. Biol.* 215 (3), 403–410.
- Arnoult, D., Soares, F., Tattoli, I., Girardin, S.E., 2011. Mitochondria in innate immunity. *EMBO Rep.* 12 (9), 901–910.
- Bayona-Bafaluy, M.P., Blits, B., Battersby, B.J., Shoubridge, E.A., Moraes, C.T., 2005. Rapid directional shift of mitochondrial DNA heteroplasmy in animal tissues by a mitochondrially targeted restriction endonuclease. *Proc. Natl. Acad. Sci. U. S. A.* 102 (40), 14392–14397.
- Bogenhagen, D.F., 2012. Mitochondrial DNA nucleoid structure. *Biochim. Biophys. Acta* 1819 (9–10), 914–920.
- Bonnard, C., Durand, A., Peyrol, S., Chanseaux, E., Chauvin, M.A., Morio, B., et al., 2008. Mitochondrial dysfunction results from oxidative stress in the skeletal muscle of diet-induced insulin-resistant mice. *J. Clin. Invest.* 118 (2), 789–800.
- Calabrese, F.M., Simone, D., Attimonelli, M., 2012. Primates and mouse NumtS in the UCSC Genome Browser. *BMC Bioinformatics* 13 (Suppl. 4), S15.
- Caro, P., Gomez, J., Arduini, A., Gonzalez-Sanchez, M., Gonzalez-Garcia, M., Borrás, C., et al., 2010. Mitochondrial DNA sequences are present inside nuclear DNA in rat tissues and increase with age. *Mitochondrion* 10 (5), 479–486.
- Chan, D.C., 2006. Mitochondria: dynamic organelles in disease, aging, and development. *Cell* 125 (7), 1241–1252.
- Falkenberg, M., Larsson, N.G., Gustafsson, C.M., 2007. DNA replication and transcription in mammalian mitochondria. *Annu. Rev. Biochem.* 76, 679–699.
- Fernandez-Vizcarra, E., Enriquez, J.A., Perez-Martos, A., Montoya, J., Fernandez-Silva, P., 2011. Tissue-specific differences in mitochondrial activity and biogenesis. *Mitochondrion* 11 (1), 207–213.
- Flicek, P., Aken, B.L., Ballester, B., Beal, K., Bragin, E., Brent, S., et al., 2010. Ensembl's 10th year. *Nucleic Acids Res.* 38 (Database issue), D557–D562.
- Goios, A., Pereira, L., Bogue, M., Macaulay, V., Amorim, A., 2007. mtDNA phylogeny and evolution of laboratory mouse strains. *Genome Res.* 17 (3), 293–298.
- Goo, H.G., Jung, M.K., Han, S.S., Rhim, H., Kang, S., 2013. HtrA2/Omi deficiency causes damage and mutation of mitochondrial DNA. *Biochim. Biophys. Acta* 1833 (8), 1866–1875.
- Green, D.R., Reed, J.C., 1998. Mitochondria and apoptosis. *Science* 281 (5381), 1309–1312.
- Guo, W., Jiang, L., Bhasin, S., Khan, S.M., Swerdlow, R.H., 2009. DNA extraction procedures meaningfully influence qPCR-based mtDNA copy number determination. *Mitochondrion* 9 (4), 261–265.

- Guo, J., Guo, Q., Fang, H., Lei, L., Zhang, T., Zhao, J., et al., 2014. Cardioprotection against doxorubicin by metallothionein is associated with preservation of mitochondrial biogenesis involving PGC-1 α pathway. *Eur. J. Pharmacol.* 737, 117–124.
- Hock, M.B., Kralli, A., 2009. Transcriptional control of mitochondrial biogenesis and function. *Annu. Rev. Physiol.* 71, 177–203.
- Liu, B., Czajka, A., Malik, A.N., Hussain, K., Jones, P.M., Persaud, S.J., 2015. Equilibrative nucleoside transporter 3 depletion in beta-cells impairs mitochondrial function and promotes apoptosis: relationship to pigmented hypertrichotic dermatosis with insulin-dependent diabetes. *Biochim. Biophys. Acta* 1852 (10 Pt A), 2086–2095.
- Malik, A.N., Czajka, A., 2013. Is mitochondrial DNA content a potential biomarker of mitochondrial dysfunction? *Mitochondrion* 13 (5), 481–492.
- Malik, A.N., Shahni, R., Iqbal, M.M., 2009. Increased peripheral blood mitochondrial DNA in type 2 diabetic patients with nephropathy. *Diabetes Res. Clin. Pract.* 86 (2), e22–e24.
- Malik, A.N., Shahni, R., Rodriguez-de-Ledesma, A., Laftah, A., Cunningham, P., 2011. Mitochondrial DNA as a non-invasive biomarker: accurate quantification using real time quantitative PCR without co-amplification of pseudogenes and dilution bias. *Biochem. Biophys. Res. Commun.* 412 (1), 1–7.
- Mercer, T.R., Neph, S., Dinger, M.E., Crawford, J., Smith, M.A., Shearwood, A.M., et al., 2011. The human mitochondrial transcriptome. *Cell* 146 (4), 645–658.
- Morscher, R.J., Aminzadeh-Gohari, S., Feichtinger, R.G., Mayr, J.A., Lang, R., Neureiter, D., et al., 2015. Inhibition of neuroblastoma tumor growth by ketogenic diet and/or calorie restriction in a CD1-Nu mouse model. *PLoS ONE* 10 (6), e0129802.
- Pearson, W.R., Lipman, D.J., 1988. Improved tools for biological sequence comparison. *Proc. Natl. Acad. Sci. U. S. A.* 85 (8), 2444–2448.
- Perier, C., Bender, A., Garcia-Arumi, E., Melia, M.J., Bove, J., Laub, C., et al., 2013. Accumulation of mitochondrial DNA deletions within dopaminergic neurons triggers neuroprotective mechanisms. *Brain* 136 (Pt 8), 2369–2378.
- Richly, E., Leister, D., 2004. NUMTs in sequenced eukaryotic genomes. *Mol. Biol. Evol.* 21 (6), 1081–1084.
- Schatz, G., 1996. The protein import system of mitochondria. *J. Biol. Chem.* 271 (50), 31763–31766.
- Stangenberg, S., Nguyen, L.T., Chen, H., Al-Odat, I., Killingsworth, M.C., Gosnell, M.E., et al., 2015. Oxidative stress, mitochondrial perturbations and fetal programming of renal disease induced by maternal smoking. *Int. J. Biochem. Cell Biol.* 64, 81–90.
- Supale, S., Thorel, F., Merkwirth, C., Gjinovci, A., Herrera, P.L., Scorrano, L., et al., 2013. Loss of prohibitin induces mitochondrial damages altering beta-cell function and survival and is responsible for gradual diabetes development. *Diabetes* 62 (10), 3488–3499.
- Wallace, D.C., Fan, W., 2009. The pathophysiology of mitochondrial disease as modeled in the mouse. *Genes Dev.* 23 (15), 1714–1736.
- Wallace, D.C., Stugard, C., Murdock, D., Schurr, T., Brown, M.D., 1997. Ancient mtDNA sequences in the human nuclear genome: a potential source of errors in identifying pathogenic mutations. *Proc. Natl. Acad. Sci. U. S. A.* 94 (26), 14900–14905.
- Williams, R.S., 1986. Mitochondrial gene expression in mammalian striated muscle. Evidence that variation in gene dosage is the major regulatory event. *J. Biol. Chem.* 261 (26), 12390–12394.
- Woischnik, M., Moraes, C.T., 2002. Pattern of organization of human mitochondrial pseudogenes in the nuclear genome. *Genome Res.* 12 (6), 885–893.
- Yao, Y.G., Kong, Q.P., Salas, A., Bandelt, H.J., 2008. Pseudomitochondrial genome haunts disease studies. *J. Med. Genet.* 45 (12), 769–772.
- Zhang, Q., Raoof, M., Chen, Y., Sumi, Y., Sursal, T., Junger, W., et al., 2010. Circulating mitochondrial DAMPs cause inflammatory responses to injury. *Nature* 464 (7285), 104–107.
- Zhao, M., Chen, X., 2014. Eicosapentaenoic acid promotes thermogenic and fatty acid storage capacity in mouse subcutaneous adipocytes. *Biochem. Biophys. Res. Commun.* 450 (4), 1446–1451.